JACS
JOURNAL OF THE AMERICAN CHEMICAL SOCIETY

COMMUNICATION

pubs.acs.org/JACS

Facet Effect of Single-Crystalline Ag_3PO_4 Sub-microcrystals on Photocatalytic Properties

Yingpu Bi, Shuxin Ouyang, Naoto Umezawa, Junyu Cao, and Jinhua Ye*

International Center for Materials Nanoarchitectonics (MANA) and Photocatalytic Materials Center, National Institute for Materials Science (NIMS), 1-2-1 Sengen, Tsukuba, Ibaraki 305-0047, Japan

Supporting Information

ABSTRACT: We recently reported that Ag_3PO_4 exhibits excellent photooxidative capabilities for O_2 evolution from water and organic dye decomposition under visible-light irradiation. However, very little is known about the shape and facet effects of Ag_3PO_4 crystals on their photocatalytic properties. Herein we have developed a facile and general route for high-yield fabrication of single-crystalline Ag_3PO_4 rhombic dodecahedrons with only {110} facets exposed and cubes bounded entirely by {100} facets. Moreover, studies of their photocatalytic performance have indicated that rhombic dodecahedrons exhibit much higher activities than cubes for the degradation of organic contaminants, which may be primarily ascribed to the higher surface energy of {110} facets (1.31 J/m^2) than of {100} facets (1.12 J/m^2).

The morphology and crystal-facet-controlled fabrication of semiconductor materials have recently attracted considerable attention because their photoelectric and photocatalytic properties can be further enhanced or optimized by tailoring the surface atomic structures.[1−4] For example, Lu and co-workers demonstrated that the {001} facets of anatase TiO_2 are much more reactive than the thermodynamically stable {101} facets for the production of H_2 from water splitting.[5−7] Moreover, it was reported that $BiVO_4$ nanoplates with exposed {100} facets exhibited enhanced photocatalytic activity for the decomposition of rhodamine B.[8] Although these highly reactive facets are more interesting and important for improving photocatalytic reactivity, they usually diminish rapidly during the growth process because of their high surface energies.[9] To address this issue, organic polymers or inorganic ions have usually been employed for selective control of the growth rates of various planes.[10,11] However, the percentage of highly reactive facets in the final products has still been relatively low. On the other hand, capping agents adsorbed on the surfaces of semiconductor crystals must be removed by complex treatments before their catalytic applications, and the highly reactive facets may lose many of their active sites as a result of surface reconstruction. Thus, the fabrication of photocatalysts with only highly reactive facets exposed and without capping agents is still a great challenge.

More recently, we reported the new use of Ag_3PO_4 semiconductor in photocatalytic applications,[12] where it exhibits extremely high photooxidative capabilities for O_2 evolution from water and organic dye decomposition under visible-light irradiation. More specifically, this novel photocatalyst can achieve quantum efficiencies of up to 90% at wavelengths greater than 420 nm, which is significantly higher than previously reported values. However, because the as-prepared Ag_3PO_4 samples possessed irregular and polyhedral crystal structures, the shape and facet effects on their photocatalytic properties have remained unclear to date. Herein we demonstrate a facile and general procedure for fabrication of single-crystalline Ag_3PO_4 rhombic dodecahedrons with only {110} facets exposed and cubes bounded by {100} facets in the absence of any capping agent. Furthermore, studies of their photocatalytic performance have clearly revealed that the rhombic dodecahedrons exhibit superior photocatalytic properties in comparison with cubes for the degradation of organic contaminants. Theoretical calculations suggest that Ag_3PO_4 {110} facets exhibit a higher surface energy than {100} planes, which may contribute significantly to the enhanced photocatalytic activity.

Figure 1A and Figure S1 in the Supporting Information show typical scanning electron microscopy (SEM) images of the Ag_3PO_4 products synthesized by simply reacting silver acetate with Na_2HPO_4 in aqueous solutions at room temperature. It can be clearly seen that all of these samples possess perfect and regular rhombic dodecahedral morphology with an average diameter of 600 nm, and some of them self-assembled into two-dimensionally ordered arrays. The enlarged SEM image (Figure 1A inset) reveals that the as-prepared Ag_3PO_4 sub-microcrystals were enclosed by 12 well-defined {110} planes with cubic crystal symmetry and single-crystal structure.[13] Interestingly, as shown in Figure 1B and Figure S2, when silver acetate was replaced by silver−ammine complex in this synthetic system, uniform Ag_3PO_4 sub-microcubes with smooth surfaces and sharp corners and edges were fabricated in large quantities. Furthermore, it can be clearly seen (Figure 1B inset) that the Ag_3PO_4 sub-microcubes were bounded completely by six square {100} facets. The basic structural units of both the Ag_3PO_4 rhombic dodecahedrons and cubes are shown in Figure S3. With extension of their facets along three-dimensional space, the corresponding large Ag_3PO_4 sub-microcrystals can be perfectly constructed. Moreover, their energy-dispersive spectroscopy (EDS) results (see Figure S4) indicate that except for the elements Cu and Zn from the supports, only Ag, O, and P elements were detected. Furthermore, the X-ray diffraction (XRD) patterns (Figure 1C) clearly show that all of the diffraction peaks of the rhombic dodecahedral and cubic samples could be indexed to the body-centered cubic structure of Ag_3PO_4 (JCPDS no. 06-0505). However, it is worth noting that obvious

Received: January 9, 2011
Published: April 12, 2011

ACS Publications © 2011 American Chemical Society

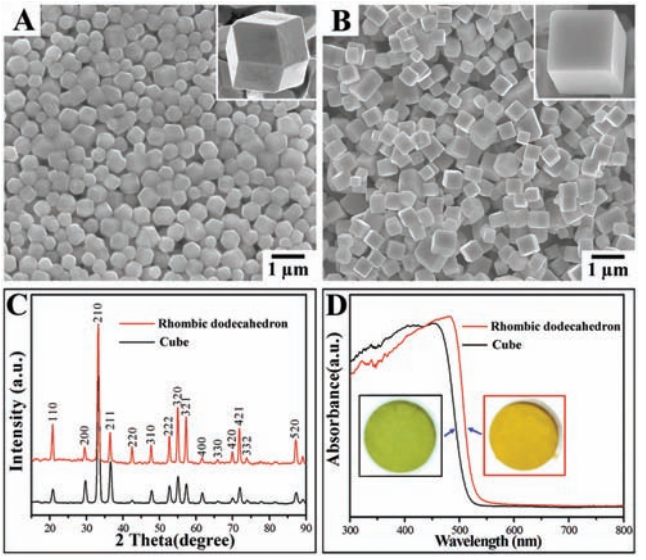

Figure 1. (A, B) SEM images of Ag_3PO_4 sub-microcrystals with different morphologies: (A) rhombic dodecahedrons; (B) cubes. (C) XRD patterns. (D) UV−vis diffusive reflectance spectra.

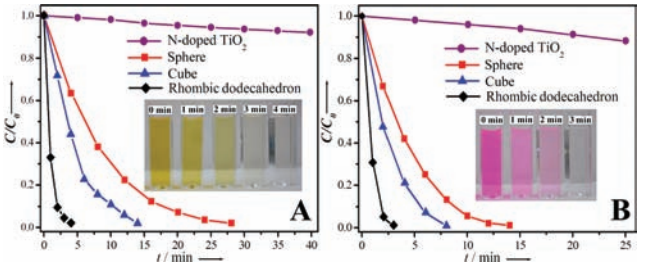

Figure 2. Photocatalytic activities of Ag_3PO_4 rhombic dodecahedrons, cubes, and spheres and N-doped TiO_2 for (A) MO and (B) RhB degradation under visible-light irradiation ($\lambda > 420$ nm).

changes in the intensity ratios for various peaks were observed, giving further support to the above SEM observations. More specifically, in the case of rhombic dodecahedrons, the intensity ratio of 2.7 for the (110) and (200) diffractions was remarkably higher than the powder intensity ratio (0.78), confirming that these crystals are primarily composed of {110} crystalline planes. In contrast, the intensity ratio for the (110) and (200) peaks for the Ag_3PO_4 cubes was only 0.52, suggesting that their surfaces are dominated by {100} planes. Their UV−vis diffuse reflectance spectra (Figure 1D) reveal that the Ag_3PO_4 rhombic dodecahedrons could absorb visible light with a wavelength shorter than 550 nm. For the Ag_3PO_4 cubes, the absorption edge was drastically shifted to around 520 nm.

Furthermore, their photocatalytic behaviors for the degradation of methyl orange (MO) and rhodamine B (RhB) dyes under visible-light irradiation were explored (Figure S9).[14] To the best of our knowledge, this is the first time that these novel Ag_3PO_4 single crystals have been used as the photocatalysts for these reactions. For comparison, the performances of spherical Ag_3PO_4 particles (Figure S10) and a commercial N-doped TiO_2 photocatalyst (Figure S11) were also investigated. As shown in Figure 2A, it can be clearly seen that unlike the N-doped TiO_2 catalyst, all of these Ag_3PO_4 photocatalysts exhibited

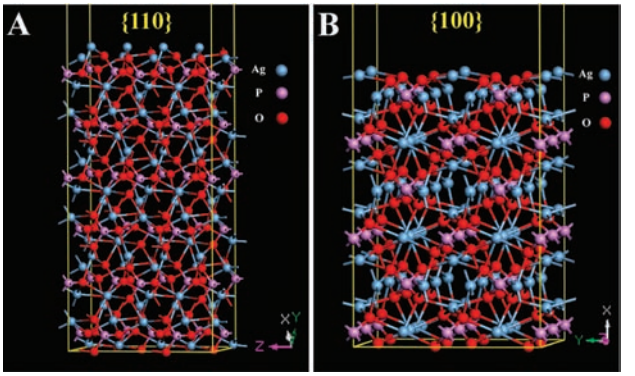

Figure 3. Relaxed geometries for the (A) {110} and (B) {100} surfaces of Ag_3PO_4 based on a 192-atom slab model. The vacuum region was set to the same thickness as Ag_3PO_4.

excellent photocatalytic activities for the MO degradation reaction. Among them, the Ag_3PO_4 rhombic dodecahedrons exhibited the highest photocatalytic activity, as they could completely degrade MO dye in 4 min under visible-light irradiation. In contrast, the cubes decomposed MO dye in 14 min, while the spherical Ag_3PO_4 particles needed ~28 min. Additionally, the experimental results for the RhB degradation under the same conditions (Figure 2B) clearly indicate that their photoreactivity order is highly consistent with the above results for the MO degradation. Furthermore, the Brunauer−Emmett−Teller adsorption analysis showed that the specific surface areas of the rhombic dodecahedrons and cubes were 2.18 and 2.32 m^2/g, respectively, clearly indicating that the significant difference in activities should not be attributed to the surface areas. Moreover, their photocatalytic performances with monochromatic visible light centered at a wavelength of 420.4 nm ($\Delta\lambda = \pm 14.9$ nm) were also investigated. As shown in Figure S12A, the light-absorption difference between Ag_3PO_4 rhombic dodecahedra and nanocubes can be eliminated under these conditions. The experimental results (Figure S12B,C) revealed that the rhombic dodecahedrons still exhibited higher photocatalytic activities than cubes for the degradation of both MO and RhB dyes. Therefore, these demonstrations indicate that the photocatalytic properties of Ag_3PO_4 sub-microcrystals can be significantly improved by tailoring the shape and surface structure.

In order to further clarify the underlying mechanism for the higher photocatalytic activity of Ag_3PO_4 rhombic dodecahedrons relative to cubes, we further studied the surface structures and surface energies of Ag_3PO_4 {100} and {110} planes through density functional theory (DFT) calculations. As shown in Figure 3, our surface models for both the {100} and {110} surfaces were constructed on the basis of a slab model including 192 atoms of Ag_3PO_4 with a vacuum region having the same thickness as Ag_3PO_4. Furthermore, each surface was cut to create a nonpolar surface, with atomic stoichiometry satisfied within the each side of the slab. Geometry relaxations were performed with the midlayers fixed. The surface energy (γ) was computed using the formula

$$\gamma = \frac{E_{slab} - nE_{bulk}}{2A}$$

where E_{slab} is the total energy of the slab, E_{bulk} is the total energy of the bulk per unit cell, n is the number of bulk unit cells contained in the slab, and A is the surface area of each side of the slab. The calculation results showed that the surface energy of {110} facets

dx.doi.org/10.1021/ja2002132 |J. Am. Chem. Soc. 2011, 133, 6490–6492

(1.31 J/m^2) is higher than that of {100} facets (1.12 J/m^2), indicating that the {110} facets should be more reactive than {100} facets. Furthermore, calculations of the surface energy of oxygen-reduced {110} and {100} facets were also performed, and the results are shown in Figure S14. It was found that oxygen vacancies can be more easily created on the {110} surface than on the {100} surface. On the basis of the above calculations, we speculate that each single-crystalline Ag_3PO_4 rhombic dodecahedron possesses 12 highly reactive {110} facets and a high density of corners, edges, and defects, which may markedly increase the number of catalytically active sites on their surfaces and facilitate the adsorption of organic molecules on these sites. Thereby, the degradation reaction between the adsorbed organic dye molecules and photogenerated holes could proceed more rapidly under visible-light irradiation, which may result in a higher photocatalytic activity for the degradation of organic dyes.

In summary, we have demonstrated a facile and efficient process for the shape-selective synthesis of uniform and perfect rhombic dodecahedral and cubic Ag_3PO_4 sub-microcrystals without using any capping agent. Moreover, studies of their photocatalytic performance have indicated that the rhombic dodecahedrons exhibit much higher catalytic activities than cubes and particles for the degradation of organic contaminants under visible-light irradiation. This fundamental understanding shows that morphological control of semiconductors allows preferential exposure of photocatalytically active facets, which will most probably be applicable in the development of highly efficient visible-light-sensitive photocatalysts.

■ ASSOCIATED CONTENT

Supporting Information. Experimental procedures, theoretical calculations, additional SEM images and EDS patterns, and additional discussion. This material is available free of charge via the Internet at http://pubs.acs.org.

■ AUTHOR INFORMATION

Corresponding Author
jinhua.ye@nims.go.jp

■ ACKNOWLEDGMENT

This work was partially supported by the World Premier International Research Center Initiative on Materials Nanoarchitectonics, MEXT, and the MEXT Program for Development of Environmental Technology Using Nanotechnology. The global COE Program of Tokyo Institute of Technology, and the Japan Society for the Promotion of Science KAKENHI (21760030).

■ REFERENCES

(1) (a) Seker, F.; Meeker, K.; Kuech, T. F.; Ellis, A. B. *Chem. Rev.* **2000**, *100*, 2505. (b) Mclaren, A.; Valdes-Solis, T.; Li, G.; Tsang, S. C. *J. Am. Chem. Soc.* **2009**, *131*, 12540. (c) Mor, G. K.; Shankar, K.; Paulose, M.; Grimes, C. A. *Nano Lett.* **2005**, *5*, 191. (d) Han, X.; Kuang, Q.; Jin, M.; Xie, Z.; Zheng, L. *J. Am. Chem. Soc.* **2009**, *131*, 3152.

(2) (a) Wang, J.; Tafen, D.; Lewis, J.; Hong, Z.; Manivannan, A.; Zhi, M.; Li, M.; Wu, N. *J. Am. Chem. Soc.* **2009**, *131*, 12290. (b) Dai, Y.; Cobley, C.; Zeng, J.; Sun, Y.; Xia, Y. *Nano Lett.* **2009**, *9*, 2455. (c) Liu, S.; Yu, J.; Jaroniec, M. *J. Am. Chem. Soc.* **2010**, *132*, 11914. (d) Lakshminarasimhan, N.; Bae, E.; Choi, W. *J. Phys. Chem. C* **2007**, *111*, 15244.

(3) (a) Choi, S.; An, K.; Kim, E.; Yu, J.; Kim, J.; Hyeon, T. *Adv. Funct. Mater* **2009**, *19*, 1645. (b) Kang, S.; Choi, S.; Kang, M.; Kim, J.; Kim, H.; Hyeon, T.; Sung, Y. *Adv. Mater.* **2008**, *20*, 54. (c) Yu, T.; Park, J.; Moon, J.; An, K.; Hyeon, T. *J. Am. Chem. Soc.* **2007**, *129*, 14558.

(4) (a) Wolcott, A.; Fitzmorris, R. K.; Muzaffery, O.; Zhang, J. Z. *Chem. Mater.* **2010**, *22*, 2814. (b) Li, G.; Dimitrijevic, N.; Chen, L.; Nichols, J.; Rajh, T.; Gray, K. A. *J. Am. Chem. Soc.* **2008**, *130*, 5402. (c) Wang, L.; Sasaki, T.; Ebina, Y.; Kurashima, K.; Watanabe, M. *Chem. Mater.* **2002**, *14*, 4827.

(5) Yang, H.; Sun, C.; Qiao, S.; Zou, J.; Liu, G.; Smith, S.; Cheng, H.; Lu, G. *Nature* **2008**, *453*, 638.

(6) Liu, G.; Sun, C.; Yang, H.; Smith, S.; Wang, L.; Lu, G.; Cheng, H. *Chem. Commun.* **2010**, *46*, 755.

(7) Liu, G.; Yang, H.; Wang, X.; Cheng, L.; Pan, J.; Lu, G.; Cheng, H. *J. Am. Chem. Soc.* **2009**, *131*, 12868.

(8) (a) Zhang, L.; Chen, D.; Jiao, X. *J. Phys. Chem. B* **2006**, *110*, 2668. (b) Xi, G.; Ye, J. *Chem. Commun.* **2010**, *46*, 1893.

(9) (a) Selloni, A. *Nat. Mater.* **2008**, *7*, 613. (b) Herman, G. S.; Sievers, M. R.; Gao, Y. *Phys. Rev. Lett.* **2000**, *84*, 3354.

(10) (a) Zhang, Z. H.; Zhong, X. H.; Liu, S. H.; Li, D. F.; Han, M. Y. *Angew. Chem., Int. Ed.* **2005**, *44*, 3466. (b) Buonsanti, R.; Grillo, V.; Carlino, E.; Giannini, C.; Kipp, T.; Cingolani, R.; Cozzoli, D. *J. Am. Chem. Soc.* **2008**, *130*, 11223. (c) Seo, J. W.; Jun, Y. W.; Ko, S. J.; Cheon, J. W. *J. Phys. Chem. B* **2005**, *109*, 5389.

(11) (a) Wen, P. H.; Itoh, H.; Tang, W. P.; Feng, Q. *Langmuir* **2007**, *23*, 11782. (b) Wu, B. H.; Guo, G. Y.; Zheng, N. F.; Xie, Z. X.; Stucky, G. D. *J. Am. Chem. Soc.* **2008**, *130*, 17563. (c) Wu, N.; Wang, J.; Tafen, D.; Wang, H.; Zheng, J.; Lewis, J.; Liu, X.; Leonard, S.; Manivannan, A. *J. Am. Chem. Soc.* **2010**, *132*, 6679.

(12) Yi, Z.; Ye, J.; Kikugawa, N.; Kako, T.; Ouyang, S.; Stuart-Williams, H.; Yang, H.; Cao, J.; Luo, W.; Li, Z.; Liu, Y.; Withers, R. *Nat. Mater.* **2010**, *9*, 559.

(13) Yang, J.; Qi, L.; Lu, C.; Ma, J.; Cheng, H. *Angew. Chem., Int. Ed.* **2005**, *44*, 598.

(14) (a) Wang, P.; Huang, B. B.; Qin, X. Y.; Zhang, X. Y.; Dai, Y.; Wei, J. Y.; Whangbo, M. H. *Angew. Chem., Int. Ed.* **2008**, *47*, 7931. (b) Wang, P.; Huang, B. B.; Zhang, X. Y.; Qin, X. Y.; Jin, H.; Dai, Y.; Wang, Z. Y.; Wei, J. Y.; Zhan, J.; Wang, S. Y.; Wang, J. P.; Whangbo, M.-H. *Chem.—Eur. J.* **2009**, *15*, 1821. (c) Bi, Y.; Ye, J. *Chem.—Eur. J.* **2010**, *16*, 10327. (d) Bi, Y.; Ye, J. *Chem. Commun.* **2009**, 6551.